Tracking land-cover changes with sedimentary charcoal in the Afrotropics

Julie C Aleman, Olivier Blarquez, Ilham Bentaleb, Philippe Bonté, Benoit Brossier, Christopher Carcaillet, Valéry Gond, Sylvie Gourlet-Fleury, Arnaud Kpolita, Irène Lefèvre, Richard Oslisly, Mitchell J Power, Olga Yongo, Laurent Bremond and Charly Favier

The Holocene 2013 23: 1853

DOI: 10.1177/0959683613508159

Research paper

The Holocene
23(12) 1853–1862

Reprints and permissions:
sagepub.co.uk/journalsPermissions.nav
DOI: 10.1177/0959683613508159
hol.sagepub.com
SAGE

Tracking land-cover changes with sedimentary charcoal in the Afrotropics

Julie C Aleman,[1,2,3,4] Olivier Blarquez,[5] Ilham Bentaleb,[4] Philippe Bonté,[6] Benoit Brossier,[1] Christopher Carcaillet,[2] Valéry Gond,[3] Sylvie Gourlet-Fleury,[3] Arnaud Kpolita,[7] Irène Lefèvre,[6] Richard Oslisly,[8] Mitchell J Power,[9] Olga Yongo,[7] Laurent Bremond[2] and Charly Favier[1]

Abstract

Fires have played an important role in creating and maintaining savannas over the centuries and are also one of the main natural disturbances in forests. The functional role of fires in savannas and forests can be investigated through examining sedimentary charcoal in order to reconstruct long-term fire history. However, the relationship between charcoal and vegetation structure in tropical grassy ecosystems remains to be elucidated. Here, we compared recent charcoal records from lake sediments in three tropical ecosystems (forest, savanna, and forest–savanna mosaic) with land cover inferred from remote-sensing images. Charcoal width-to-length (W/L) ratio is a good proxy for changes in fuel type. At one of the lakes, a significant W/L modification from values >0.5 (mainly wood) to <0.5 (-grass) was recorded simultaneously with changes in land cover. Indeed, a significant deforestation was recorded around this lake in the remote-sensing imagery between 1984 and 1994. The results also indicate that a riparian forest around a lake could act as a physical filter for charcoal accumulation; we used the mean charcoal size as a proxy to evaluate this process. Charcoal Accumulation Rates (CHAR), a burned biomass proxy, were combined with W/L ratio and the mean charcoal size to investigate the land-use history of the landscapes surrounding the study sites. This combined approach allowed us to distinguish between episodic slash-and-burn practices in the forest and managed fields or pastures burning frequently.

Keywords

agriculture, Central African Republic, charcoal morphology, charcoal taphonomy, forest, lake, methodology, paleoecology, savanna, sedimentary charcoal

Received 25 April 2013; revised manuscript accepted 9 August 2013

Introduction

Every year, there are more fires in the tropics than anywhere else on Earth, which is an important source of global carbon and black carbon emissions (Van der Werf et al., 2010). The flammability of tropical forests is low compared to adjacent open vegetation such as savannas or pasture (Hoffmann et al., 2012). Nevertheless, human land use has increasingly changed the wildfire regimes, as a result of forest fragmentation caused by logging and agriculture (e.g. Cochrane, 2003; Laporte et al., 2007; Laurance et al., 2001), particularly by modifying the conductibility of forest edges with respect to fire spread (e.g. Bucini and Lambin, 2002; Cochrane et al., 1999). Likewise, savannas are increasingly subject to intense human pressure (Solbrig et al., 1996), and fires are mainly of anthropogenic origin related to hunting, managing livestock pastures, and controlling pests and other wildlife threats. Furthermore, burning of forest and savanna is frequently undertaken to create and extend new agricultural areas (Ickowitz, 2006; Kotto-Same et al., 1997). Given the modifications of human land use on tropical landscapes (e.g. Cochrane, 2009), understanding and quantifying both recent and past fire activities are crucial to forecast and model changes in biomass burning emissions (Van der Werf et al., 2013).

Charcoal records are used in long-term ecological studies as proxies for biomass burning (Carcaillet et al., 2002; Power et al., 2008) and for fire regime reconstruction (e.g. Blarquez et al., 2013; Clark, 1988; Whitlock and Larsen, 2001). Most methodological studies that examine the link between charcoal and fire were conducted in the temperate and boreal regions (e.g. Blackford, 2000; Clark, 1988; Clark et al., 1998; Enache and Cumming, 2006; Peters and Higuera, 2007; Tinner et al., 2006; Whitlock and Millspaugh, 1996); only a few studies are available covering tropical or subtropical regions, in either open or closed ecosystems (Duffin et al., 2008). In contrast to temperate, boreal, or mountain ecosystems, fire-return intervals (FRI) in tropical savanna and in disturbed forests are generally short (between 1 and 10 years; Archibald et al. (2010)).

[1]Centre Nationale de la Recherche Scientifique, France
[2]École Pratique des Hautes Études, France
[3]Centre de coopération internationale en recherche agronomique pour le développement (CIRAD), France
[4]Université Montpellier 2, France
[5]Université du Québec à Montréal (UQAM), Canada
[6]Commissariat à l'énergie atomique et aux énergies alternatives, France
[7]Université de Bangui, Central African Republic
[8]Institut de Recherche pour le Développement (IRD), Gabon
[9]University of Utah, USA

Corresponding author:
Julie C Aleman, Centre for Bio-Archaeology and Ecology (UMR5059/CNRS, Université Montpellier 2, EPHE), 163 rue Auguste Broussonet, Institut de Botanique, 34090 Montpellier, France.
Email: julie.aleman@univ-montp2.fr

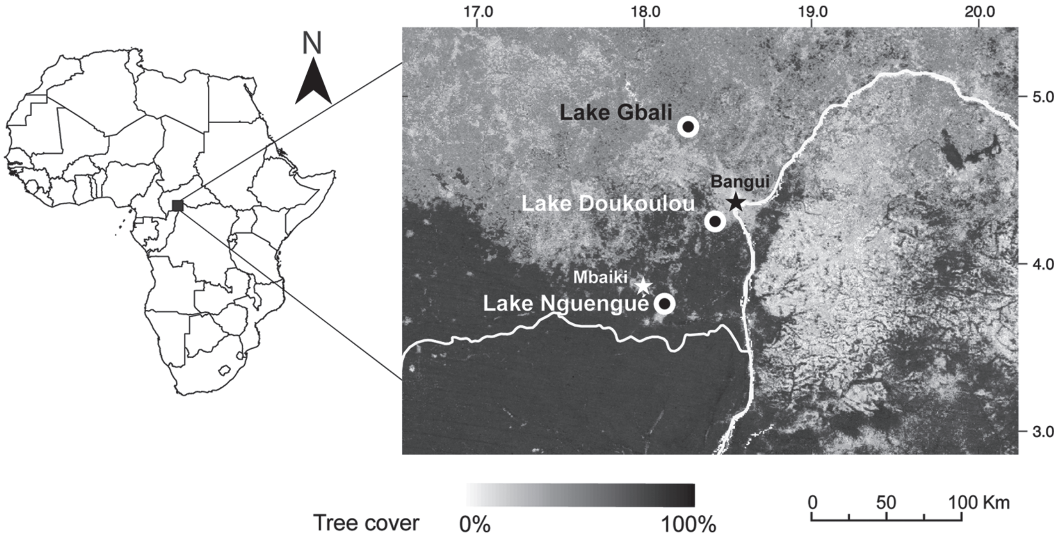

Figure 1. Location of the three lakes in the Central African Republic on a map showing tree cover (extracted from the Vegetation Continuous Fields product of MODIS V3 (Hansen et al., 2003)).

Unfortunately, the sampling resolution of lake sediments is generally lower than the FRI, which hinders detection of individual fire events (Nelson et al., 2012). For these reasons, a calibration framework was established to enable fire area and intensity in South African savannas to be investigated from sedimentary charcoal records (Duffin et al., 2008). However, these calibrations might not be applicable to other tropical regions because of significant differences between fuel types due to variations in the biomass productivity and grasses composition (e.g. O'Connor, 1994). The biomass type could be reconstructed through width-to-length (W/L) ratio of charcoal (Umbanhowar and Mcgrath, 1998). Gillson and Ekblom (2009) and Ekblom and Gillson (2010) separated elongated charcoal particles on pollen-slides to examine the change in fuel type; however, the significance of this ratio with land cover was not calibrated. In such a context, there is a need to better understand how sedimentary charcoal can be used in tropical ecosystems to reconstruct fire history, both in herb- and tree-dominated landscapes. Moreover, the role of fire in initiating and maintaining tropical savannas is still debated (e.g. Bond et al., 2005; Gillson, 2004; Staver et al., 2011), and there is a need for long-term tropical fire reconstructions that can be used to decipher fire–vegetation relationships.

Our study investigated the potential of several proxies based on sedimentary charcoal records for fire history reconstructions from three lakes in Central Africa, located in forest, forest–savanna mosaics, and savanna. We analyzed Charcoal Accumulation Rates (CHAR) expressed in terms of both number of particles and area, as commonly used in paleofire studies (Mooney and Tinner, 2011; Power et al., 2008). We also evaluated the potential of charcoal W/L ratios and mean charcoal size as proxies for fire reconstruction. It is known that different charcoal morphology results from different source material (Enache and Cumming, 2006; Jensen et al., 2007). We hypothesize that the morphology of charcoal expressed as W/L would directly mirror the fuel type (Umbanhowar and Mcgrath, 1998). A decrease in the W/L ratios of charcoal fragments should indicate that grasses represent the main burned fuel type. We test the robustness of these proxies against the land-cover changes around each lake assessed using satellite images from 1974 to 2005.

Materials and methods

Study sites

Three lakes in the Central African Republic were selected, located in three different ecosystems, that is, savanna, forest–savanna mosaic, and forest. The savanna lake, Lake Gbali (4°49′07″N, 18°15′46″E; Figure 1) is a 2-ha shallow lake with a gently sloping bottom (2 m depth on the sampling date). The surrounding woody savanna, within 1 km around the lake, is composed of a grass sward dominated by *Imperata cylindrica* (L.) Raeusch associated with *Cenchrus polystachios* (L.) Morrone and *Hyparrhenia diplandra* (Hack.) Stapf. The woody cover contains typical fire-resistant trees, that is, *Daniellia oliveri* (Rolfe) Hutch. and Dalz., *Terminalia schimeriana* Hochst., *Prosopis africana* (Guill. & Perr.) Taub., *Hymenocardia acida* Tul., *Piliostigma thonningii* (Schumach.) Milne-Redh., *Sarcocephalus latifolius* (Sm.) E.A. Bruce, *Annona senegalensis* Pers., and *Crossopteryx febrifuga* (Afzel. ex G.Don) Benth. There is a 200-m-wide riparian forest that is mainly composed of *Hallea stipulosa* (DC.) Leroy and some *Raphia vinifera* P. Beauv.

The forest–savanna lake, Lake Doukoulou (4°15′10″N, 18°25′25″E; Figure 1), is surrounded by a mosaic of densely wooded savanna (*I. cylindrica, Vetiveria zizanioides* L. Nash, and *Pennisetum purpureum* Schumach. in the herb strata, and *P. thonningii, Erythrina sigmoidea* Hua, *Vitex doniana* Sweet., *Terminalia glaucescens*, and very sparse *D. oliveri, Albizia zygia* (DC.) J.F. Macbr., in the woody strata) and very degraded forest (*Terminalia superba* Engl. & Diels, *Cola lateritia* K. Schum., and *Pycnanthus angolensis* (Welw.) Warb. with *Chromolaena odorata* (L.) R.M. King & H. Rob, which is an alien invasive species). This is a 36-ha lake with a gently sloping bottom (depth 2.35 m) surrounded by an extensive zone dominated by Poaceae with a gradation of *V. zizanioides, I. cylindrica*, and *P. purpureum* from the edge of the lake toward the savanna.

Lake Nguengué (3°45′40″N, 18°07′19″E; Figure 1) is located in a mature semi-evergreen forest (containing *Celtis tessmannii* Rendle, *Trilepisium madagascariense* DC., *Pentaclethra macrophylla* Benth., *Pouteria altissima* (A.Chev.) Baehni, *Triplochiton scleroxylon* K. Schum., *Macaranga barteri* Müll. Arg., and *Myrianthus arboreus* P. Beauv.), which is affected by human activity, as attested by the presence of ruderal trees (*Elaeis guineensis* Jacq., *P. angolensis*, and *Musanga cecropioides* R.Br.). It is a 14-ha lake with a gently sloping bottom (2.30 m depth) within a wide riparian forest essentially composed of *Alstonia boonei* De Wild., with scattered *H. stipulosa* and *Raphia farinifera* (Gaertn.) Hyl.

The Lake Gbali and Lake Doukoulou experience a tropical climate with annual precipitation of about 1500 mm, alternating between a 4-month dry season from November to February, followed by an 8-month long wet season (Bangui weather station; Hijmans et al., 2009). The Lake Nguengué is located in an area with a shorter dry season (December to February), and the climate is wetter with an average annual rainfall of 1738 mm (1982–2007 period, Boukoko Meteorological Station, A Ougou, personal communication, 2008).

Sampling and sediment dating

In each lake, cores of the topmost water-saturated sediments were extracted in December 2010 using a Kajak-Brinkhurst sampler. Lake Gbali, Lake Doukoulou, and Lake Nguengué core depths were of 42, 15, and 33 cm, respectively, and were sliced into contiguous layers, each 1 cm thick. Dating of the sediment was based on radioactive cosmogenic tracer analysis, ^{7}Be (half-life = 53.22 days) and ^{210}Pb (half-life = 22.3 years; Appleby and Oldfieldz, 1992), which are preferentially and strongly attached to fine particles (Gallon et al., 2006; Grousset et al., 1999). Both are gamma emitters and can be detected in small amounts of sediment (about 100 g), without any previous chemical treatment. Sediment content analysis of each radioactive element was carried out using gamma spectrometry (e.g. Le Cloarec et al., 2011; San Miguel et al., 2005). For the top four 1-cm sections, we established an age–depth model using the decomposition of ^{7}Be (Eq. (1)) and for the remainder of each core, we used ^{210}Pb decomposition (Eq. (2)) based on a constant initial concentration (CIC) model (Appleby and Oldfieldz, 1992). This model assumes that the supply of ^{210}Pb to the sediment is proportional to the sedimentation rate and, thus, will change in response to changes in sediment flux. Application of the CIC model was considered justified on the basis of the smooth exponential decline of $^{210}Pb_{unsup}$ concentrations when plotted against accumulated dry mass (O'Reilly et al., 2011). The age T_m of the sediment layer is given by Eq. (1) for the top 4 cm and by Eq. (2) for the rest of the core:

$$T_m = T_0 - \frac{1}{\lambda_1} \times \ln\left(\frac{^{7}Be^{0}}{^{7}Be^{m}}\right) \quad (1)$$

$$T_m = T_0 - \frac{1}{\lambda_2} \times \ln\left(\frac{^{210}Pb^{0}_{unsp}}{^{210}Pb^{m}_{unsp}}\right) \quad (2)$$

where T_0 is the age of the first stratigraphic level, λ_1 is the decay constant for ^{7}Be (λ_1 = 4.754 per year), $^{7}Be^{0}$ is the value of ^{7}Be in the first stratigraphic level, $^{7}Be^{m}$ is the value of ^{7}Be in layer m, λ_2 is the decay constant for ^{210}Pb ($\lambda_2 = 3.12 \times 10^{-2}$ per year), $^{210}Pb^{0}$ is the unsupported ^{210}Pb value for the first layer, and $^{210}Pb^{m}$ is the value for the layer m.

Charcoal analysis

Cores were sampled contiguously in 1-cm layers for the charcoal analyses. The entire 1-cm core slice (~44 cm^3) was analyzed when the sediment was too water saturated: 0–11 cm depth for Lake Doukoulou, 0–14 cm depth for L. Gbali, and 0–15 cm depth for Lake Nguengué. Only 1 cm^3 was analyzed when the sediment was sufficiently solid. The samples were soaked in a 5% KOH solution to deflocculate particles and bleached in a 10% solution of NaOCl and passed through a 160-µm mesh to collect macroscopic charcoals (Carcaillet et al., 2001). Due to the high content of organic matter, meshes containing the charcoal particles were soaked for 24 h in a 33% solution of hydrogen peroxide (H_2O_2). Charcoal particles were analyzed under a stereomicroscope coupled to a digital camera and image-analysis software to calculate the area, length, and width of each particle. For each sample, we estimated (1) charcoal influx values (CHARs) using the ^{210}Pb age–depth models, both in terms of number ($CHAR_n$ in particles/cm^2/yr) and surface area ($CHAR_a$ in mm^2/cm^2/yr); (2) sample average charcoal area (mm^2); and (3) sample average W/L ratio of charcoal particles (no units).

We assumed that grasses would produce elongated particles and their associated W/L would be <0.5, whereas woody material would produce squarer charcoal particles and the W/L would be >0.5 (Umbanhowar and Mcgrath, 1998). Although Umbanhowar and Mcgrath (1998) used a length-to-width (L/W) ratio that could produce values approaching infinity when W is close to 0, we found it more convenient to use the inverse ratio, for which the value is $0 < W/L \leq 1$ (1 = square particle).

Remote-sensing data analysis

We used Landsat Multispectral Scanner (MSS; 68 m × 83 m pixel resolution) and Thematic Mapper (TM, 30 m pixel resolution) images collected in January 1974, December 1984, December 1994, January 1995, and February 1999, and SPOT 5 images (2.5 m pixel resolution) from December 2005. We identified two vegetation classes, the first corresponding to closed vegetation, that is, forest, and the second to open landscape: savanna, fields, and pastures have similar spectral signatures. Likewise, it was not possible to distinguish reliably between savanna types based on their different tree covers (Favier et al., 2012). These two vegetation classes are expected to support contrasting fuel types: savanna, fields, and pastures are chiefly characterized by grass fuels, whereas woody fuels dominate in forests. The two classes were delimited using supervised classification (minimum distance algorithm) in ENVI 4.3 using 10 areas of homogeneous land cover for the training data. We visualized images in 'natural colors' using a composite image from Landsat bands 5-4-3 (see detailed methodology in online Appendix). To evaluate the changes in land cover, and then in potential fuel type, for each image and around each lake, we computed the percentages of forested pixels at different distances from the lake center (1–10 km). Indeed, charcoal particles >160 µm best reflect fire at a scale <1 km in a forested environment (e.g. Clark et al., 1998; Lynch et al., 2004) and probably <10 km in an open one (Duffin et al., 2008).

Statistical analysis

Confidence interval (CI) values for each proxy were computed by bootstrap resampling the mean 10,000 times. We used an analysis of variance (ANOVA) to assess the significance of the difference in $CHAR_n$ and $CHAR_a$ between the periods highlighted within each lake. Between lakes, differences in mean charcoal particle size were assessed using a Kruskal–Wallis test. W/L ratio frequencies were presented using normalized histograms for each sample. The normalization involved transforming data using minimax transformation. All analyses were done under MATLAB R2012a, codes and data are available on request to the corresponding author.

Results

Age–depth models

For Lake Gbali, the dates derived from ^{210}Pb are well defined according to the restricted CI (Figure 2a); the modeled ages cover the period AD 1916–2010 for the depth 0–40 cm. In Lake Doukoulou, for the depth 0–20 cm, the modeled ages (Figure 2b) cover the period AD 1900–2010. Finally, in Lake Nguengué, the deepest sediments (22–33 cm depth) exhibited an inversion of dates that is associated with very large CI, making the age–depth model inaccurate for depths greater than 22 cm (Figure 2c). In this lake, the charcoal analyses were not undertaken for samples predating

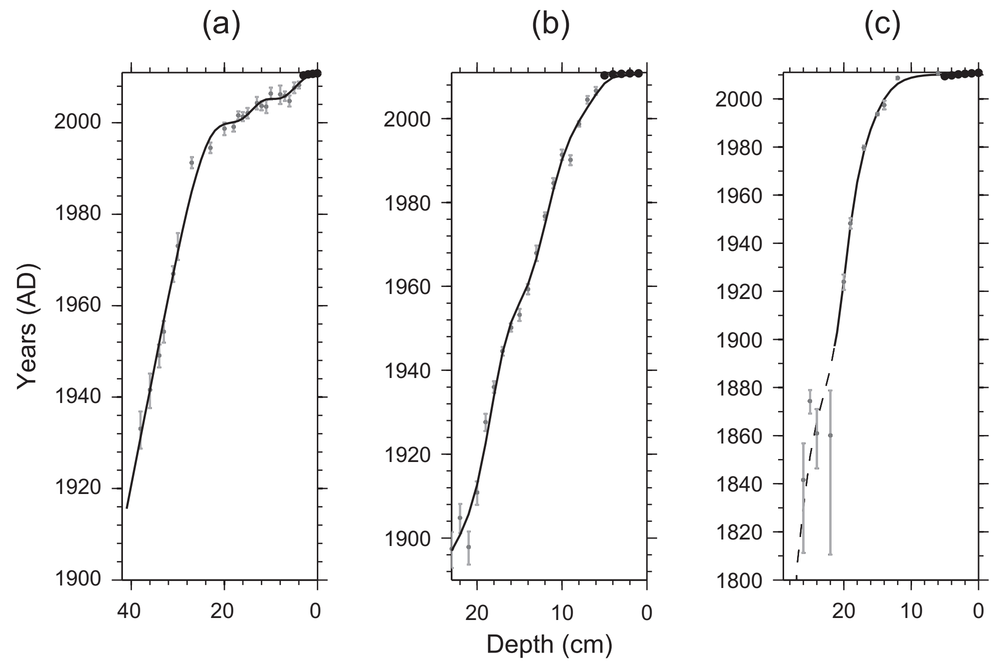

Figure 2. Computed age–depth model (CIC) represented by solid lines for the three lakes. The dates are inferred from measured ^{210}Pb (gray points and error-bars) and ^{7}Be (black points and error-bars smaller than the dots). (a) Lake Gbali, (b) Lake Doukoulou, and (c) Lake Nguengué. CIC: constant initial concentration.

AD 1900, and the age range of this lake is AD 1900–2010. For the three lakes, the charcoal analyses and the resulting fire reconstructions covered most of the 20th century until AD 2010, the last year before the sampling.

CHAR

Within each lake, $CHAR_a$ and $CHAR_n$ displayed parallel trends (Figure 3a–c). For Lake Gbali (Figure 3a), $CHAR_n$ ranged between 1.34 and 182.90 [min, max] particles/cm^2/yr and $CHAR_a$ between 0.04 and 7.67 mm^2/cm^2/yr. There were three different temporal phases associated with the CHAR values (Table 1): from AD ~1910 to AD ~1960, CHAR values were stable; from AD ~1970–2000, there was a general increase; and after AD 2000, a clear decrease. For Lake Doukoulou (Figure 3b), $CHAR_n$ and $CHAR_a$ values were in the ranges 0.87–33.47 particles/cm^2/yr and 0.06–4.14 mm^2/cm^2/yr, respectively. There was no significant change in CHAR along the sequence (Table 1). For Lake Nguengué (Figure 3c), $CHAR_n$ and $CHAR_a$ values were associated with four temporal phases. Between AD ~1900 and AD ~1950, CHAR values were very low: $CHAR_n$ was on average ~0.11 particles/cm^2/yr and $CHAR_a$ was ~0.01 mm^2/cm^2/yr (Table 1). The first increase in CHAR values was recorded between AD ~1960 and AD 1990, then a plateau occurred between AD ~1990 and the beginning of the 2000s, and a second increase was recorded after this. The values of CHAR during this last increase reached values similar to those of Lake Doukoulou and the recent part of the Lake Gbali sequence (on average 13.41 [8.15, 21.31] (95% CI) particles/cm^2/yr and 0.79 [0.47, 1.31] mm^2/cm^2/yr; Table 1).

Mean charcoal fragment size

In Lake Gbali, the average size of charcoal fragments for the whole sequence was 0.0494 [0.0475, 0.0517] mm^2 (Table 2). The deviation around this average was low until 1990, after which the variability in charcoal size increased (Figure 3d). For Lake Doukoulou, the average size of the charcoal fragments was 0.1174 [0.1127, 0.1242] mm^2 (Figure 3e). From AD ~1940 to AD ~1970, the fragments were smaller, but a trend of increasing mean charcoal size was observed. Finally, in Lake Nguengué, the average charcoal size was 0.0565 [0.0530, 0.0611] mm^2 (Table 2). Lake Doukoulou charcoal fragments were larger than the fragments recorded in the other two lakes (Kruskal–Wallis test; Table 2).

W/L ratio

In Lake Gbali, W/L values were consistently lower than 0.5 (Figure 3g). In Lake Doukoulou, there was an abrupt change in W/L ratio between AD ~1983 and AD ~1990. Before AD ~1983, the W/L was around 0.7, values dropped to around 0.4 after AD ~1990 (Figure 3h). In Lake Nguengué, the W/L ratio was highly variable before AD ~1960 with no significant changes detected since there were insufficient charcoal particles per sample for robust statistical analysis. After 1960, the ratio stabilized around values lower than 0.5 (Figure 3i).

Land-cover transformation

Around Lake Gbali, the landscape has remained covered with a wooded savanna with forest galleries since the 1970s (Figure 4b–d): in the image analysis, the percentages of forest pixels within 5 km of the center of the lake were lower than 30% (Figure 4a). Any change in savanna tree cover aside, the landscape around Lake Gbali has, therefore, not changed significantly since at least AD 1974. Within a radius of 1 km from the lake center, the highest numbers of forest pixels were found, indicating the presence of dense riparian forest. Beyond the 1-km radius, we found no significant difference in the amount of forest between the other distances tested (2–10 km from the center of the lake; Figure 4a).

Lake Doukoulou's surroundings changed abruptly from a forest to a more open landscape between AD 1984 and AD 1994 (Figure 4f–h). In AD 1974 and AD 1984, the numbers of forest pixels were similar for all the distances examined (Figure 4e), whereas in AD 1999, there was a clear difference between what was recorded within the first 3 km (*c*. 40% forest pixels) and 10 km from the center of the lake (*c*. 68%).

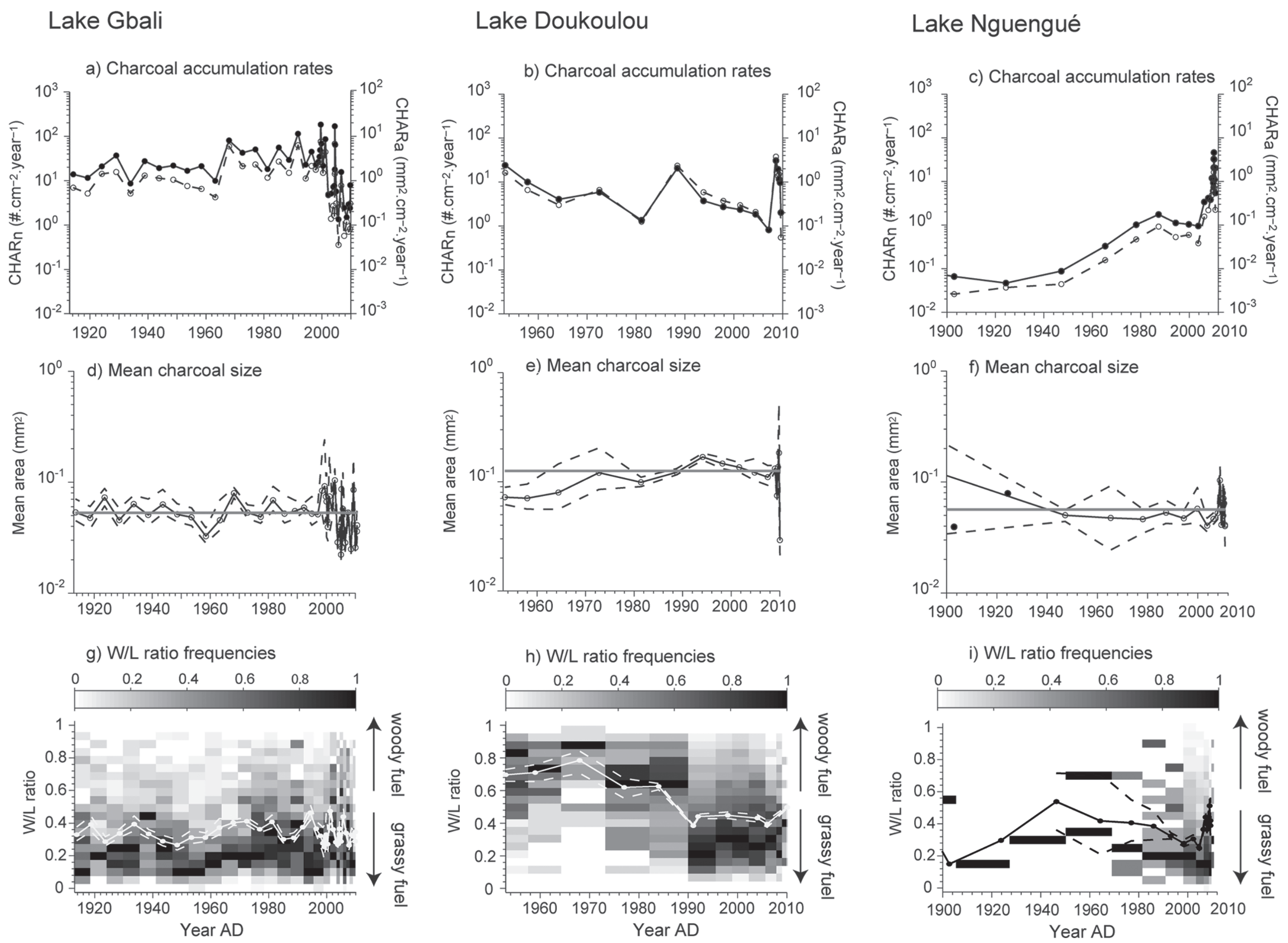

Figure 3. Charcoal accumulation rates with respect to number and area ($CHAR_n$, solid lines, and $CHAR_a$, dotted lines) for (a) Lake Gbali, (b) Lake Doukoulou, and (c) Lake Nguengué represented using a logarithmic scale. Mean charcoal particle size computed by averaging the charcoal area per sample (mean $CHAR_a$, open points and black solid line), (d, e, and f) 90% bootstrapped CI (dotted lines) and mean $CHAR_a$ for the whole sequence (gray line) for the three lakes. (f) For Lake Nguengué, the solid points represent samples with only one charcoal particle. W/L ratio frequencies normalized to the most frequent value (values from 0 to 1 represented in shades of gray), the average W/L (white line for Gbali and Doukoulou, black line for Nguengué), and 90% bootstrapped CI (dotted white lines for Gbali and Doukoulou, dotted black lines for Nguengué) for each sample for the three lakes (g, h, and i).
W/L: width to length.

Table 1. Summary of $CHAR_n$ and $CHAR_a$ for the three lakes. $mCHAR_n$ is the mean CHAR number along the whole sedimentary sequence, 95 CI $CHAR_n$ is the bootstrapped 95% CI of $CHAR_n$, $mCHAR_a$ is the mean CHAR area along the whole sedimentary sequence, and 95 CI $CHAR_a$ is the bootstrapped 95% CI of $CHAR_a$. Significant differences within site based on ANOVA ($p < 0.05$) are indicated by lower case letters (a ≠ b ≠ c).

Lake name	Period	$mCHAR_n$ (particles/cm²/yr)	95 CI $CHAR_n$	$mCHAR_a$ (mm²/cm²/yr)	95 CI $CHAR_a$
Gbali	~1910–1960	25.54[a]	[18.39, 40.54]	1.39[a]	[0.92, 2.68]
	~1970–2000	55.17[b]	[86.69, 39.07]	2.89[b]	[2.13, 4.06]
	~2002–2010	21.00[a,c]	[7.09, 64.11]	0.84[a,c]	[0.31, 2.64]
Doukoulou	~1950–1983	9.84[a]	[4.17, 21.28]	0.73[a]	[0.37, 1.56]
	~1990–2010	10.44[a]	[5.21, 17.99]	1.21[a]	[0.61, 2.13]
Nguengué	~1900–1950	0.11[a]	[0.08, 0.19]	0.01[a]	[0.005, 0.03]
	~1960–1990	0.89[b]	[0.45, 1.29]	0.05[b]	[0.02, 0.07]
	~1995–2010	13.41[c]	[8.15, 21.31]	0.79[c]	[0.47, 1.31]

CI: confidence interval; CHAR: Charcoal Accumulation Rate; ANOVA: analysis of variance.

Table 2. Comparison of mean charcoal particle size for the three lakes. The mean charcoal size represents the averaged charcoal areas for the whole sedimentary sequence. The 95% CIs were computed using 10,000 bootstrapped estimates of the mean. Significant differences based on the Kruskal–Wallis test are indicated by lower case letters (a ≠ b ≠ c).

Lake name	Mean charcoal size (mm²)	95% CI
Gbali	0.0494[a]	[0.0475, 0.0517]
Doukoulou	0.1174[b]	[0.1127, 0.1242]
Nguengué	0.0565[c]	[0.0530, 0.0611]

CI: confidence interval.

Around Lake Nguengué, the dense forest landscape experienced an expansion of open patches between AD 1974 and AD 1994, shown by the gradual decrease in forest pixel percentages within 5 km of the lake center (95–78%; Figure 4i). These patches of open vegetation were clearly distinguishable in 5-4-3 Landsat image composites. They correspond to fields and pastures (Figure 4j–l).

W/L ratio versus land-cover

The land-cover type (forest versus non-forest) around the three lakes was compared with W/L patterns representing fuel type. Around Lake Gbali, during the past three decades, the landscape has consistently comprised woody savanna vegetation with grasses as the main fuel type, and accordingly, the W/L was stable and <0.5 (Figure 4a).

The area around Lake Doukoulou experienced a land-cover transformation that was initiated between AD 1984 and AD 1994 and continues today. Deforestation occurred mainly from the northeast (Figure 4f and g). Over the whole of the area investigated, the percentage of forest pixels in the Landsat images dropped from 90% to 65% between AD 1984 and AD 1994 (Figure 4e). However, within a radius of 5 km from the lake center, the forest area dropped from 65% to 45% between AD 1994 and AD 1999. Between these dates, the percentage of forest pixels dropped, but the actual number differed according to the distance from the center of the lake. The W/L ratio was coherent with land-cover changes assessed from remote-sensing images with a ratio >0.5 up to AD ~1983 and then a decrease (Figure 4e).

At Lake Nguengué between AD ~1970 and AD 2010, the W/L ratio was <0.5 (Figure 4i), which is coherent with remote-sensing images indicating a stable forest matrix with open vegetation patches (Figure 4j–l).

Discussion

We aimed to investigate the potential of CHAR number and area, W/L ratio, and mean charcoal fragment size to reconstruct long-term fire history by comparing the modern charcoal records of three lakes situated in three different vegetation zones with their surrounding vegetation during the last three decades based on remote sensing. We showed that changes in the charcoal records matched the transformation in land cover. The following paragraphs discuss the respective relevance of the charcoal parameters we used to assess the transformation of land-cover.

Sedimentary charcoal and land-cover change

In Lake Gbali, surrounded by a woody savanna since the 1970s, the W/L values for the whole sequence were less than 0.5, which corresponds to grass as the main fuel type (Umbanhowar and Mcgrath, 1998). The values of $CHAR_n$ were higher than those from other sedimentary records of savanna ecosystems (Duffin, 2008; Nelson et al., 2012), probably because around Lake Gbali, the grass cover is more productive in terms of biomass and would produce more charcoal particles (see next discussion section). But these differences could also result from taphonomic processes that control the flux of particles from the catchment area of the lake basin. The increase in CHAR numbers and areas from the 1960s onward can be explained by the settlement of a farmers' community between the late 1950s and the late 1970s (Benoit-Janin, 1957; Boulvert, 1983) that probably resulted in the establishment and expansion of agricultural fields, as attested by the visual comparison of the aerial photographs from 1952 and 1960. Since the late 1990s, $CHAR_n$ and $CHAR_a$ (Figure 3a) have decreased, and their values are lower than during the rest of the sequence, although there is no obvious change in land-cover (Figure 4a–d). However, the 30-m resolution of the land-cover analysis is too low to detect small-scale changes in savanna tree density. A visual comparison of higher resolution images, that is, mid-1960s aerial photographs (declassified satellite images from Earth Explorer) and recent Google Earth images, indicates an increase in tree cover, probably due to less frequent fires, which could explain the recent decrease in CHAR values (Archibald et al., 2009). This tree cover increase and the potential reduction in burned areas or fire occurrences can be explained by the recent abandonment of villages around Lake Gbali; this is due to political instability and road deterioration since few years.

At Lake Doukoulou, the timing of the deforestation coincides with the increasing demand for domestic wood from the city of Bangui during the late 1980s (Boulvert, 1990). Moreover, before AD 1990, the W/L ratio indicates that wood was the main fuel for vegetation fires, which may reflect slash-and-burn activities (Bruzon, 1994; Cochrane, 2009). These land-use changes corresponded to the charcoal peak dated AD ~1990 and associated with low W/L ratios (Figure 3b), indicating deforestation and burning of grass biomass. Nevertheless, the CHAR values were comparable before and after deforestation, and there was no correlation

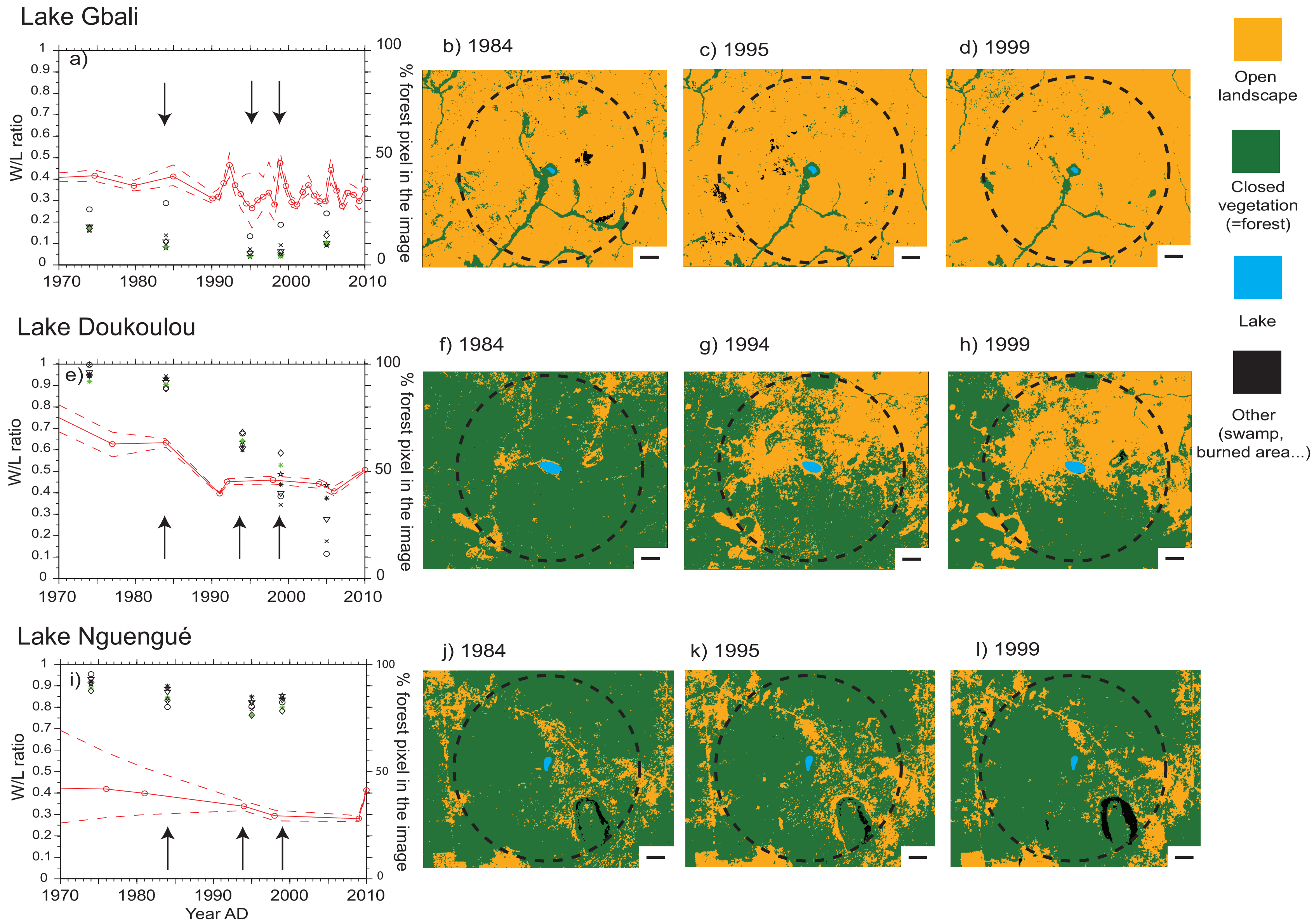

Figure 4. Comparison of the W/L ratio (red line: mean, dotted lines: 95% CI) and the percentages of forested pixels from the land cover analysis for the three lakes (a, e, and i). Various distances from the lake center were analyzed: ○1 km, ×2 km, ▽3 km, *4 km, *5 km, *7 km, and ◇10 km. There are no data from 2005 for the Lake Nguengué area because of the presence of clouds in the Landsat image. (b, f, and j) Maps of land cover classification for the three lakes are shown for 1984, (g) 1994 for Lake Doukoulou or 1995 for (c) Lake Gbali and (k) Lake Nguengué (d, h, and l) and 1999. The arrows in panels (a), (e), and (i) correspond to these three images. The black lines on the maps correspond to 1 km, and the lake is represented in blue at the center of each map, the circles of dotted lines have a 5 km radius from the center of the lake. CI: confidence interval; W/L: width to length.

between the distance from the lake center and changes in charcoal, since the absolute location of fires could not be determined.

The W/L data from Lake Nguengué were difficult to assess from AD 1900 to AD 1950 because of the very low charcoal abundance. After AD 1950, W/L reached a value lower than 0.5 and the CI also decreased. These low W/L ratios were associated with increasing CHAR corresponding to an increase in grass burning. The first part of the CHAR increase coincides with the beginning of logging followed by the establishment of rubber and coffee plantations in the area from the late 1940s onward; these activities were associated with an increase in human population density. Forest disturbance increased recently with the intensification of logging in the 1990s (Laporte et al., 2007) and the development of the town of Bobengua Bouchia. Increasing connectivity of fields and pastures (Figure 4j–l), probably maintained by setting fires (Bruzon, 1994; Laris, 2002), was associated with increased population density and increasing demands for resources. This increase in land use is obvious in the high-resolution images from 2006 and 2011 available through Google Earth software and reflects the same changes documented in the Lake Nguengué charcoal record and the recent increase in CHAR values (Figure 3c).

Interpreting charcoal records

CHAR. Changes in CHAR values in the sediments correlate with observed changes in burned biomass. Indeed, in Lake Nguengué, there is an obvious increase in CHAR values since AD ~1940, with CHAR in the same range as those of Lake Doukoulou and Lake Gbali for the period AD 2002–2010 (Table 1). Thus, CHAR recorded in a lake situated in a forest matrix containing fields and pastures is similar to CHAR in a savanna matrix. In this context, CHAR represents a proxy of the burned biomass and, indirectly, of agriculture.

We also observed that the CHAR number for Lake Gbali was higher than from other sedimentary records from savanna ecosystems, whatever the period analyzed. For example, Nelson et al. (2012) found $CHAR_n$ values less than 5.0 particles/cm^2/yr on average for the whole sequence, covering the last 25,000 years in Lake Chala (East Africa), whereas $CHAR_n$ values for Lake Gbali and Lake Doukoulou were, on average, 25.9 and 7.4 particles/cm^2/yr, respectively (calculated for charcoal particles with length >255 µm, diagonal length of a 180-µm mesh to be comparable to Nelson et al. (2012) study). Lake Chala is situated in a semi-arid environment with annual rainfall below ~800 mm, whereas Lake Gbali and Lake Doukoulou are situated in an area receiving about 1500 mm/yr. The main difference could be due to lower biomass productivity related to annual rainfall (Clark et al., 2001; O'Connor, 1994; Ohiagu and Wood, 1979), but also to other mechanisms that limit biomass productivity (soil), charcoal productivity (e.g. fire frequency from two fires per year to one fire per 10 years), or charcoal taphonomy (patterns in the catchment area). For their study, $CHAR_a$ data are not available, but their values are expected to be lower than for Lake Gbali and Lake Doukoulou due to the correlation between $CHAR_n$ and $CHAR_a$ (Tinner and Hu (2003) and Carcaillet (2007) if fragmentation processes are limited (Leys et al., 2013), and for our three lakes, the R^2 between $CHAR_n$ and $CHAR_a$ was >0.85 (data not shown)). $CHAR_a$ values from Mt Muhavura crater lake and Mt Gahinga crater swamp peaked at respectively 0.8 and 0.2 mm^2/cm^2/yr. These maximum values are likewise generally inferior to those observed in Lake Gbali except during the 2000s (McGlynn et al., 2013).

In our study area, high rainfall would support a higher tall-grass biomass and a higher fire frequency (once or twice a year). Consequently, the vegetation must be characterized when fire is reconstructed based on $CHAR_n$ (and $CHAR_a$) in order to determine whether the charcoal flux is related to the biomass grass type, for example, using phytolith assemblages to distinguish tall-grass from short-grass savannas (Bremond et al., 2008). However, grazing also constitutes a mechanism that reduces grass biomass by promoting small lawn-grass species (Archibald et al., 2005) and, consequently, creates a fuel deficit (Van Langevelde et al., 2003).

Mean size of charcoal fragments. We found that the mean size of charcoal fragments deposited in Lake Doukoulou was twice that in Lake Gbali and Lake Nguengué. The main difference between the vegetation around the three lakes in their watersheds is the presence of a large riparian forest around Gbali and Nguengué, whereas Doukoulou is surrounded by a large marsh mainly composed of Poaceae. The riparian forest would represent a physical filter for wind transport of charcoal. It has been shown that convection during fire causes turbulence that suspends particles in the combustion zone and that thermal buoyancy provides the energy needed to loft particles above the canopy (Clark, 1988; Peters and Higuera, 2007). In that case, only small-sized charcoal particles would be transported above the riparian forest and deposited in the lake. In contrast, when the riparian forest is absent, large charcoal particles can be deposited by wind (Whitlock and Larsen, 2001) or directly by runoff (Carcaillet et al., 2007). A further argument for this explanation is the change over time of the mean charcoal particle sizes at Doukoulou. Before AD 1978, the mean size was less than 0.1 mm^2, which would indicate the occurrence of a physical filter. Indeed, before the 1980s, the lake was situated in a forest and the trees around the lake would have acted as a filter for charcoal input into the lake, even if the grassy area right on the edge of the lake was already well established.

Thus, the routine investigation of mean size of charcoal particles in tropical sediments can be relevant for paleofire reconstruction, highlighting the contraction or expansion of riparian forest around a sediment coring site and also the importance of physical (and thus taphonomic) filters.

W/L ratio. The W/L ratio constitutes a powerful tool for paleofire analyses since it allows the fuel type to be distinguished (Umbanhowar and Mcgrath, 1998). It has previously been shown that charcoal morphology could constitute an interesting technique to identify fuel type and yield important insights into fire reconstructions from temperate and boreal ecosystems (Enache and Cumming, 2006; Jensen et al., 2007), and this study establishes it for tropical ones. Furthermore, W/L ratio represents a strong complement to CHAR analysis since both permit inferences about the land use in the area around the lake. Indeed, high CHAR values combined with a W/L <0.5 in a forest area would indicate that fire fuel included both grasses and wood. In long-term sedimentary sequences, CHAR values combined with W/L ratios could provide clues to understanding structural changes in savanna ecosystems or forest disturbance regimes, whether or not they were associated with land-use changes.

Conclusion

By comparing land-cover with sedimentary charcoal records, we showed that it is possible to reconstruct biomass burning history in tropical biomes using charcoal records by combining CHAR and W/L ratio values. Indeed, burned grass vegetation produces a signal that can be interpreted on the basis of charcoal morphology (W/L ratio), reflecting the main fuel type, whether grass or wood. Furthermore, the pattern of CHAR number and area reveals changes in biomass burned or fire occurrences: CHAR values increased with the establishment of fields and pastures, demonstrating that biomass burning and landscape arrangement more favorable for ignition and fire spread are associated with positive feedbacks.

Studying both vegetation cover through remote sensing and charcoal particle accumulation in accurately dated lake sediments allowed us to make a comparison between charcoal patterns and the history of the areas around the lakes, thus allowing robust interpretation of the data. We inferred a fire history from the charcoal records expressed in terms of burned biomass that is related to the fire extent but also to the distance from the lake. We stress the need for accurate measurements of charcoal features, that is, mean charcoal size and W/L ratio, for future paleofire reconstruction in tropical sedimentary records.

Acknowledgements

We warmly thank Laurent Dezileau (Geosciences Montpellier) for his comments on the age–depth models and two anonymous reviewers for constructive comments.

Funding

This study was financially supported by the French National Research Agency (ANR, 2008-29489-62704-33) through the ErA Net BiodivERsA CoForChange project to SGF and the CNRS-PICS Inter-Tropical Fires project to CC. We acquired SPOT images through the ISIS program. The PhD thesis of JCA is co-supported by the French CNRS, CIRAD, and EPHE; supervised by CC and SGF; and guided by CF and LB.

References

Appleby P and Oldfieldz F (1992) *Application of Lead-210 to Sedimentation Studies. Uranium Series Disequilibrium, Application to Earth, Marine and Environmental Sciences*. Oxford: Clarendon Press, pp. 731–778.

Archibald S, Bond W, Stock W et al. (2005) Shaping the landscape: Fire-grazer interactions in an African savanna. *Ecological Applications* 15: 96–109.

Archibald S, Nickless A, Govender N et al. (2010) Climate and the inter annual variability of fire in southern Africa: A meta analysis using long term field data and satellite derived burnt area data. *Global Ecology and Biogeography* 19: 794–809.

Archibald S, Roy DP, van Wilgen BW et al. (2009) What limits fire? An examination of drivers of burnt area in southern Africa. *Global Change Biology* 15: 613–630.

Benoit-Janin P (1957) *Etude pédologique des blocs 3-B et 4 du paysannat de Kouzindoro et des terrains bordant la route Boutili-Kouzindoro (Ombella-M'Poko)*. Bangui: ORSTOM.

Blackford J (2000) Charcoal fragments in surface samples following a fire and the implications for interpretation of subfossil charcoal data. *Palaeogeography, Palaeoclimatology, Palaeoecology* 164: 33–42.

Blarquez O, Girardin MP, Leys B et al. (2013) Paleofire reconstruction based on an ensemble-member strategy applied to sedimentary charcoal. *Geophysical Research Letters* 40: 2667–2672.

Bond W, Woodward F and Midgley G (2005) The global distribution of ecosystems in a world without fire. *New Phytologist* 165: 525–538.

Boulvert Y (1983) *Roches carbonatées et modèle karstique en Centrafrique: aperçus historique, géologique, morphologique, phytogéographique, zoologique et hydrologique sur la caractérisation et l'extension des formations carbonatées centrafricaines*. Paris: ORSTOM.

Boulvert Y (1990) *Avancée ou recul de la forêt centrafricaine: Changements climatiques, influence de l'homme et notamment des feux*. In: Lanfranchi R and Schwartz D (eds) *Paysages quaternaires de l'Afrique centrale atlantique*. Paris: ORSTOM, pp. 353–366.

Bremond L, Alexandre A, Peyron O et al. (2008) Definition of grassland biomes from phytoliths in West Africa. *Journal of Biogeography* 35: 2039–2048.

Bruzon V (1994) Les pratiques du feu en Afrique subhumide, exemple des milieux savanicoles de la Centrafrique et de la Côte d'Ivoire. In: Blanc Pamard C and Boutrais J (eds) *À la croisée des chemins*. Paris: ORSTOM, pp. 147–163.

Bucini G and Lambin EF (2002) Fire impacts on vegetation in central Africa: A remote-sensing-based statistical analysis. *Applied Geography* 22: 27–48.

Carcaillet C (2007) Charred particle analysis. In: Elias S (ed.) *Encyclopedia of Quaternary Science*. Amsterdam: Elsevier, pp. 1582–1593.

Carcaillet C, Almquist H, Asnong H et al. (2002) Holocene biomass burning and global dynamics of the carbon cycle. *Chemosphere* 49: 845–863.

Carcaillet C, Bouvier M, Fréchette B et al. (2001) Comparison of pollen-slide and sieving methods in lacustrine charcoal analyses for local and regional fire history. *The Holocene* 11: 467–476.

Carcaillet C, Perroux A-S, Genries A et al. (2007) Sedimentary charcoal pattern in a karstic underground lake, Vercors massif, French Alps: Implications for palaeo-fire history. *The Holocene* 17: 845–850.

Clark JS (1988) Particle motion and the theory of charcoal analysis: Source area, transport, deposition, and sampling. *Quaternary Research* 30: 67–80.

Clark JS, Grimm EC, Lynch J et al. (2001) Effects of Holocene climate change on the C4 grassland/woodland boundary in the northern plains, USA. *Ecology* 82: 620–636.

Clark JS, Lynch J, Stocks BJ et al. (1998) Relationships between charcoal particles in air and sediments in west-central Siberia. *The Holocene* 8: 19–29.

Cochrane M (2009) *Tropical Fire Ecology: Climate Change, Land Use and Ecosystem Dynamics*. Berlin and Heidelberg: Springer.

Cochrane MA (2003) Fire science for rainforests. *Nature* 421: 913–919.

Cochrane MA, Alencar A, Schulze MD et al. (1999) Positive feedbacks in the fire dynamic of closed canopy tropical forests. *Science* 284: 1832–1835.

Duffin K (2008) The representation of rainfall and fire intensity in fossil pollen and charcoal records from a South African savanna. *Review of Palaeobotany and Palynology* 151: 59–71.

Duffin K, Gillson L and Willis K (2008) Testing the sensitivity of charcoal as an indicator of fire events in savanna environments: Quantitative predictions of fire proximity, area and intensity. *The Holocene* 18: 279–291.

Ekblom A and Gillson L (2010) Hierarchy and scale: Testing the long term role of water, grazing and nitrogen in the savanna landscape of Limpopo National Park (Mozambique). *Landscape Ecology* 25: 1529–1546.

Enache MD and Cumming BF (2006) Tracking recorded fires using charcoal morphology from the sedimentary sequence of Prosser Lake, British Columbia (Canada). *Quaternary Research* 65: 282–292.

Favier C, Aleman J, Bremond L et al. (2012) Abrupt shifts in African savanna tree cover along a climatic gradient. *Global Ecology and Biogeography* 21: 787–797.

Gallon C, Tessier A, Gobeil C et al. (2006) Historical perspective of industrial lead emissions to the atmosphere from a Canadian smelter. *Environmental Science & Technology* 40: 741–747.

Gillson L (2004) Evidence of hierarchical patch dynamics in an East African savanna? *Landscape Ecology* 19: 883–894.

Gillson L and Ekblom A (2009) Untangling anthropogenic and climatic influence on riverine forest in the Kruger National Park, South Africa. *Vegetation History and Archaeobotany* 18: 171–185.

Grousset F, Jouanneau J, Castaing P et al. (1999) A 70 year record of contamination from industrial activity along the Garonne River and its tributaries (SW France). *Estuarine, Coastal and Shelf Science* 48: 401–414.

Hansen M, DeFries R, Townshend J et al. (2003) Global percent tree cover at a spatial resolution of 500 meters: First results of the MODIS vegetation continuous fields algorithm. *Earth Interactions* 7: 1–15.

Hijmans R, Cameron S and Parra J (2009) WorldClim – Global climate data. Available at: http://www.worldclim.org.

Hoffmann WA, Geiger EL, Gotsch SG et al. (2012) Ecological thresholds at the savanna–forest boundary: How plant traits, resources and fire govern the distribution of tropical biomes. *Ecology Letters* 15: 759–768.

Ickowitz A (2006) Shifting cultivation and deforestation in tropical Africa: Critical reflections. *Development and Change* 37: 599–626.

Jensen K, Lynch EA, Calcote R et al. (2007) Interpretation of charcoal morphotypes in sediments from Ferry Lake, Wisconsin, USA: Do different plant fuel sources produce distinctive charcoal morphotypes? *The Holocene* 17: 907–915.

Kotto-Same J, Woomer PL, Appolinaire M et al. (1997) Carbon dynamics in slash-and-burn agriculture and land use alternatives of the humid forest zone in Cameroon. *Agriculture, Ecosystems & Environment* 65: 245–256.

Laporte NT, Stabach JA, Grosch R et al. (2007) Expansion of industrial logging in central Africa. *Science* 316: 1451.

Laris P (2002) Burning the seasonal mosaic: Preventative burning strategies in the wooded savanna of southern Mali. *Human Ecology* 30: 155–186.

Laurance WF, Cochrane MA, Bergen S et al. (2001) Environment: The future of the Brazilian Amazon. *Science* 291: 438–439.

Le Cloarec MF, Bonte P, Lestel L et al. (2011) Sedimentary record of metal contamination in the Seine River during the last century. *Physics and Chemistry of the Earth, Parts A/B/C* 36: 515–529.

Leys B, Carcaillet C, Dezileau L et al. (2013) A comparison of charcoal measurements for reconstruction of Mediterranean paleo-fire frequency in the mountains of Corsica. *Quaternary Research* 79: 337–349.

Lynch J, Clark J and Stocks B (2004) Charcoal production, dispersal, and deposition from the Fort Providence experimental fire: Interpreting fire regimes from charcoal records in boreal forests. *Canadian Journal of Forest Research* 34: 1642–1656.

McGlynn G, Mooney S and Taylor D (2013) Palaeoecological evidence for Holocene environmental change from the Virunga volcanoes in the Albertine Rift, central Africa. *Quaternary Science Reviews* 61: 32–46.

Mooney S and Tinner W (2011) The analysis of charcoal in peat and organic sediments. *Mires & Peat* 7: Article 9 (pp. 1–18).

Nelson DM, Verschuren D, Urban MA et al. (2012) Long-term variability and rainfall control of savanna fire regimes in equatorial East Africa. *Global Change Biology* 18: 3160–3170.

O'Connor T (1994) Composition and population responses of an African savanna grassland to rainfall and grazing. *Journal of Applied Ecology* 155–171.

Ohiagu C and Wood T (1979) Grass production and decomposition in Southern Guinea savanna, Nigeria. *Oecologia* 40: 155–165.

O'Reilly J, Vintró LL, Mitchell P et al. (2011) 210 Pb-dating of a lake sediment core from Lough Carra (Co. Mayo, western Ireland): Use of paleolimnological data for chronology validation below the 210 Pb dating horizon. *Journal of Environmental Radioactivity* 102: 495–499.

Peters ME and Higuera PE (2007) Quantifying the source area of macroscopic charcoal with a particle dispersal model. *Quaternary Research* 67: 304–310.

Power M, Marlon J, Ortiz N et al. (2008) Changes in fire regimes since the Last Glacial Maximum: An assessment based on a global synthesis and analysis of charcoal data. *Climate Dynamics* 30: 887–907.

San Miguel EG, Pérez-Moreno JP, Bolivar JP et al. (2005) Efficiency calibration for 210Pb gamma spectrometric determinations in sediment samples. *Radioactivity in the Environment* 7: 166–174.

Solbrig OT, Medina E and Silva J (1996) *Biodiversity and Tropical Savanna Properties: A Global View* (Scope-Scientific Committee on Problems of the Environment International Council of Scientific Unions 55). Chichester: John Wiley & Sons, pp. 185–211.

Staver AC, Archibald S and Levin S (2011) Tree cover in sub-Saharan Africa: Rainfall and fire constrain forest and savanna as alternative stable states. *Ecology* 92: 1063–1072.

Tinner W and Hu FS (2003) Size parameters, size-class distribution and area-number relationship of microscopic charcoal: Relevance for fire reconstruction. *The Holocene* 13: 499–505.

Tinner W, Hofstetter S, Zeugin F et al. (2006) Long-distance transport of macroscopic charcoal by an intensive crown fire in the Swiss Alps-implications for fire history reconstruction. *The Holocene* 16: 287–292.

Umbanhowar CE and Mcgrath MJ (1998) Experimental production and analysis of microscopic charcoal from wood, leaves and grasses. *The Holocene* 8: 341–346.

Van der Werf GR, Peters W, van Leeuwen T et al. (2013) What could have caused pre-industrial biomass burning emissions to exceed current rates? *Climate of the Past* 9: 289–306.

Van der Werf GR, Randerson JT, Giglio L et al. (2010) Global fire emissions and the contribution of deforestation, savanna, forest, agricultural, and peat fires (1997–2009). *Atmospheric Chemistry and Physics* 10: 11707–11735.

Van Langevelde F, Van De Vijver C, Kumar L et al. (2003) Effects of fire and herbivory on the stability of savanna ecosystems. *Ecology* 84: 337–350.

Whitlock C and Larsen C (2001) Charcoal as a fire proxy. In: Smol JP, Birks HJB and Last WM (eds) *Tracking Environmental Change Using Lake Sediments*. Dordrecht: Kluwer Academic Publishers, pp. 75–97.

Whitlock C and Millspaugh SH (1996) Testing the assumptions of fire-history studies: An examination of modern charcoal accumulation in Yellowstone National Park, USA. *The Holocene* 6: 7–16.